SCIENCE CHINA
Physics, Mechanics & Astronomy

• Research Paper •

July 2010 Vol.53 No.7: 1339–1347
doi: 10.1007/s11433-010-4027-9

Hydroelastic dynamic characteristics of a slender axis-symmetric body

CHEN WeiMin[1], LI Min[2*], ZHENG ZhongQin[1] & ZHANG LiWu[1]

[1] *Laboratory of Environmental Mechanics, Institute of Mechanics, Chinese Academy of Sciences, Beijing 100190, China;*
[2] *School of Aeronautics Sciences and Technology, Beijing University of Aeronautics and Astronautics, Beijing 100191, China*

Received December 10, 2009; accepted April 21, 2010; published online June 7, 2010

The slender axis-symmetric submarine body moving in the vertical plane is the object of our investigation. A coupling model is developed where displacements of a solid body as a Euler beam (consisting of rigid motions and elastic deformations) and fluid pressures are employed as basic independent variables, including the interaction between hydrodynamic forces and structure dynamic forces. Firstly the hydrodynamic forces, depending on and conversely influencing body motions, are taken into account as the governing equations. The expressions of fluid pressure are derived based on the potential theory. The characteristics of fluid pressure, including its components, distribution and effect on structure dynamics, are analyzed. Then the coupling model is solved numerically by means of a finite element method (FEM). This avoids the complicacy, combining CFD (fluid) and FEM (structure), of direct numerical simulation, and allows the body with a non-strict ideal shape so as to be more suitable for practical engineering. An illustrative example is given in which the hydroelastic dynamic characteristics, natural frequencies and modes of a submarine body are analyzed and compared with experimental results. Satisfactory agreement is observed and the model presented in this paper is shown to be valid.

hydroelasticity, added mass, vibration, frequency, mode

PACS: 02.70.Dh, 46.40.Jj, 46.40.Ff, 47.15.km

1 Introduction

Hydroelasticity is a branch of science concerned with the motion of deformable solid bodies through liquids [1–4]. For a hydroelastic system hydrodynamic force depends on and conversely influences the displacement, velocity and acceleration of solid body motion. This interaction works as a coupling between fluid and the inertia, elasticity and damping of a solid body. Consequently the concepts of added variable, i.e. added mass, added stiffness and added damping respectively produced by inertia coupling, elasticity coupling and damping coupling in the fluid field, are proposed. To solve these added variables, depending on the fluid field and boundary condition on the interface between liquids and solid body, is very difficult. It is one of the important subjects in the hydroelasticity domain.

A moving submarine elastic body, such as a submarine-launched missile experiencing a series of stages: emission from canister launcher, submarine motion and emergence from water surface, usually faces problems due to fluid-structure interactions such as dynamic response, hydroelastic divergence/flutter and kinematical stability. In order to improve structure performance, that is, long sailing distance and powerful attack ability, in the missile design stage, dynamic/static strength calculation and structure optimization are required. Therefore accurate hydroelastic dynamic characteristics, i.e. frequency and mode shape, should be primarily calculated. The methods for analyzing dynamic characteristics of marine bodies can be classified into two kinds. One kind is called simplified method [5–8], by which the fluid- structure interaction is considered added

*Corresponding author (email: limin@buaa.edu.cn)

mass whose value is determined analytically by the potential flow theory for some special bodies with an ideal shape. For example, the added mass coefficient is 1 for a cylinder and 1/2 for a sphere. In the alternative method [9–14] the dynamics of fluid-structure coupling system are computed by means of direct numerical simulation, i.e.. the synthesis method combining CFD and FEM or the generalized finite element method (GFEM) where fluid is regarded as equivalent solid and the techniques originally for solid mechanics are generalized to the coupling system in which displacements of solid and fluid are employed as basic independent variables [15]. The simplified method is good for the body with an ideal shape, but in practical engineering many structures have complex and non-ideal geometry shape. Direct numerical simulation, requiring data communication between solid and fluid software and mesh match or interpolation, is time consuming and inconvenient, and by now has not been applied to practical engineering. Moreover for GFEM where displacement variable is used to describe fluid dummy, zero energy modes may be produced since the ideal fluid is treated as a solid whose shear stiffness is zero [16]. To eliminate these zero energy modes is very complicated.

In this paper the slender axis-symmetric body moving in water is taken as the object of study. A coupling model taking account of interactions between hydrodynamic forces and structure dynamic forces is developed, where displacement of a solid body (including rigid motion and elastic deformation) and fluid pressure are employed as basic independent variables. The fluid pressure expressions are derived. Characteristics of fluid pressure, including its components, distribution and effect on structure dynamics, are analyzed. Then the coupling model is solved numerically by means of the finite element method (FEM). This avoids the complicacy, combining CFD (fluid) and FEM (structure), of direct numerical simulation and allows the body with a non ideal geometry shape so as to be suitable for practical engineering. An illustrative example is given in which the hydroelastic dynamic characteristics, i.e. natural frequencies and modes, of a body moving in water are analyzed and compared with experimental results. Satisfactory agreement is observed and the model presented in this paper is shown to be valid.

2 Analysis model

2.1 Basic equations

The deformation of solid body is assumed to satisfy Euler beam condition, and the fluid is ideal, incompressible and in infinite space. The coordinate systems are shown in Figure 1. *XYZ* is inertial coordinate. *xyz* is relative coordinate, fixed on the moving body, whose original point is consistent with the mass center of solid body. The *x*-*z* plane parallels the *X*-*Z* plane. Only the motion in the *X*-*Z* plane is considered

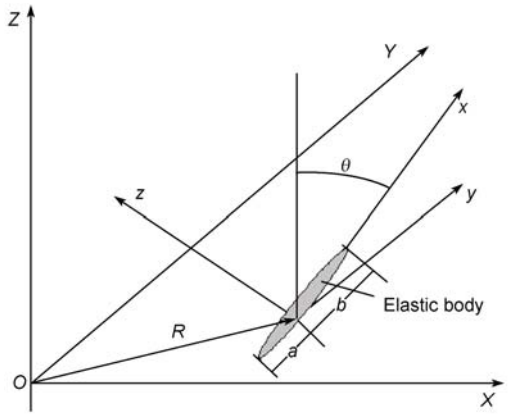

Figure 1 Sketch of the coordinate systems.

here. *X* and *Z* denote translation displacements of body mass center and ϑ is the rotation angle of a rigid body in the inertia coordinate system, and *u* and *w* denote displacements, respectively in the axial and transverse direction, in the *xyz* coordinate system. The coordinate $\overline{r}$ and motion velocity $\dot{\overline{r}}$ of structure point *i* are $\overline{r}_i = \overline{R} + \overline{\rho}_i$ and $\dot{\overline{r}}_i = \dot{\overline{R}} + \overline{\omega} \times \overline{\rho}_i + \dot{\overline{\rho}}_i$ respectively, where

$$\overline{R} = (X \sin\vartheta + Z\cos\vartheta)\overline{i} + (-X\cos\vartheta + Z\sin\vartheta)\overline{k},$$

$$\overline{\rho}_i = (x_i + u_i + \alpha z_i)\overline{i} + y_i\overline{j} + (z_i + w_i)\overline{k},$$

$\overline{i}, \overline{j}, \overline{k}$ are unit vectors respectively in the direction of the x, y, z axis, $\overline{\omega}$ is the rotation angle velocity of rigid body rotation, and $\alpha = \partial w/\partial x$.

System kinetic energy is written as

$$\begin{aligned} K &= \frac{1}{2}\sum m_i \dot{\overline{r}}_i \cdot \dot{\overline{r}}_i \\ &= \frac{1}{2}\sum m_i \Big[\dot{\overline{R}} \cdot \dot{\overline{R}} + (\overline{\omega} \times \overline{\rho}_i) \cdot (\overline{\omega} \times \overline{\rho}_i) \\ &\quad + \dot{\overline{\rho}}_i \cdot \dot{\overline{\rho}}_i + 2(\overline{\omega} \times \overline{\rho}_i) \cdot \dot{\overline{\rho}}_i \Big]. \end{aligned}$$

And system potential energy is

$$\begin{aligned} U = &\frac{1}{2}\iiint E\left(x, \sqrt{y^2+z^2}\right)\left(\frac{\partial u}{\partial x} + z\frac{\partial \alpha}{\partial x}\right)^2 \mathrm{d}x\mathrm{d}y\mathrm{d}z \\ &- \frac{1}{2}\iiint E\left(x, \sqrt{y^2+z^2}\right)\frac{\partial u}{\partial x}\left(\frac{\partial w}{\partial x}\right)^2 \mathrm{d}x\mathrm{d}y\mathrm{d}z. \end{aligned}$$

Given the gravity field effect, the gravity potential energy can be included in the system potential energy as a form of $-\sum m_i \overline{g} \cdot (\overline{R} + \overline{\rho}_i) = MgZ$, where M is the total structure mass.

An arbitrary point on the structure surface is described by the coordinate (x, γ), where γ is the circumferential angle from the z axis (Figure 2). The fluid forces exerted on

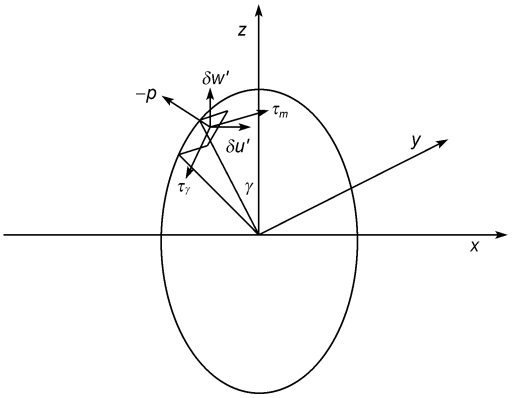

Figure 2 Forces and displacements on the surface element.

the surface element $\mathrm{d}A = (a(x)/\cos\phi(x))\mathrm{d}x\mathrm{d}\gamma$, where $a(x)$ is the radius of section x and $\phi(x)$ is the meridian slope (Figure 3), consist of pressure $p(x,\gamma)$, shear stress $\tau_m(x,\gamma)$ tangent to the meridian surface and shear stress $\tau_\gamma(x,\gamma)$ tangent to the circumferential cross section (Figure 3). The virtual displacements, described by $\delta u'$ (in the x direction) and $\delta w'$ (in the z direction), are decomposed into normal and tangential components and multiply the corresponding stress. Then the virtual work exerted on the surface element is

$$\mathrm{d}\delta W = \frac{a(x)}{\cos\phi(x)}\mathrm{d}x\mathrm{d}y(-p\overline{n} + \tau_\gamma\overline{e}_r + \tau_m\overline{e}_m)\cdot(\delta u'\overline{i} + \delta w'\overline{k}),$$

where $\overline{n},\overline{e}_r,\overline{e}_m$ are unit vectors in the normal, circumferential and meridian direction. Integrating the above equation can yield the virtual work exerted on the cross section.

Substituting kinetic energy K, potential energy U and virtual work δW into the Hamilton theorem

$$\delta\int_0^t (K-U)\mathrm{d}t + \int_0^t \delta w\mathrm{d}t = 0,$$

and applying the variational principle, yields the governing equations of structure kinematics and dynamics taking into account of fluid forces acting on the structure (neglecting the surface shear stress and higher order terms containing α) as follows:

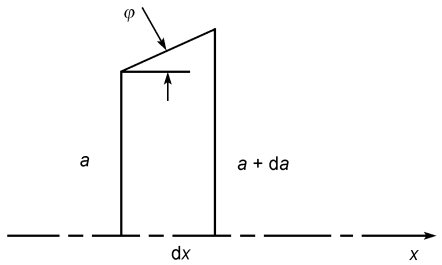

Figure 3 Segment of the axis-symmetric body.

$$M\frac{\mathrm{d}^2X}{\mathrm{d}t^2} = \int_{-a}^{b} a(x)\left(\sin\vartheta\tan\phi\int_0^{2\pi} p\mathrm{d}\gamma + \cos\vartheta\int_0^{2\pi} p\cos\gamma\mathrm{d}\gamma\right)\mathrm{d}x, \tag{1a}$$

$$M\frac{\mathrm{d}^2Z}{\mathrm{d}t^2} = \int_{-a}^{b} a(x)\left(\cos\vartheta\tan\phi\int_0^{2\pi} p\mathrm{d}\gamma - \sin\vartheta\int_0^{2\pi} p\cos\gamma\mathrm{d}\gamma\right)\mathrm{d}x - Mg, \tag{1b}$$

$$J\frac{\mathrm{d}^2\vartheta}{\mathrm{d}t^2} = \int_{-a}^{b} a(x)[-a(x)\tan\phi + x]\int_0^{2\pi} p\cos\gamma\mathrm{d}\gamma\mathrm{d}x + \int_{-a}^{b} m\left(w\frac{\mathrm{d}^2u}{\mathrm{d}t^2} - u\frac{\mathrm{d}^2w}{\mathrm{d}t^2}\right)\mathrm{d}x, \tag{1c}$$

and

$$m\frac{\partial^2u}{\partial t^2} + m\frac{\partial\vartheta}{\partial t}\frac{\partial w}{\partial t} = K(x)\frac{\partial^2u}{\partial x^2} - \frac{1}{2}\frac{\partial}{\partial x}K(x)\left(\frac{\partial w}{\partial x}\right)^2 + a(x)\tan\phi\int_0^{2\pi} p\mathrm{d}\gamma, \tag{2a}$$

$$m\frac{\partial^2w}{\partial t^2} - m\frac{\partial\vartheta}{\partial t}\frac{\partial u}{\partial t} = \frac{\partial^2}{\partial x^2}\left[H(x)\frac{\partial^2w}{\partial x^2}\right] - \frac{\partial}{\partial x}K(x)\frac{\partial u}{\partial x}\frac{\partial w}{\partial x} - a(x)\int_0^{2\pi} p\cos\gamma\mathrm{d}\gamma, \tag{2b}$$

where J is the inertia moment, m is the structure mass per unit length. $H(x) = \iint z^2E(x,\sqrt{y^2+z^2})\mathrm{d}y\mathrm{d}z$ and $K(x) = \iint E(x,\sqrt{y^2+z^2})\mathrm{d}y\mathrm{d}z$ respectively correspond to the bending and tension stiffness.

Since the fluid pressure $p(\gamma,x)$ depends on the structure motions, eqs. (1) and (2) indicate the interaction between the structure motion and the fluid dynamics. The second term on the right-hand side of eq. (1c) and the second terms on the left-hand side of eqs. (2a) and (2b) show that the rigid motion couples with the elastic deformation vibration. Eqs. (1) and (2) should be solved by time steps, since the differential/integral equations can not be separately solve due to the fluid-structure interaction.

The static hydraulic pressure terms in eqs. (1) and (2) can be derived respectively as: zero, ρgV, $-\rho gVx_b\sin\vartheta$, $-2\pi\rho ga(Z_c + x\cos\vartheta)\tan\phi$ and $\pi a^2\rho g\sin\vartheta$. V is the body volume, x_b is the distance from the buoyancy center to the mass center along the symmetric axis. Z_c is the value of the Z coordinate of mass center in the inertial coordinates.

Since the static hydraulic pressure has been known, p denotes only dynamic hydraulic pressure in later sections.

2.2 Expressions for hydrodynamic pressure

Potential function Φ of ideal incompressible fluid satisfies Laplace equation $\nabla^2\Phi=0$. And from the integral form, $p=-\rho\dfrac{\partial\Phi}{\partial t}-\dfrac{1}{2}\rho(\nabla\Phi)^2-\rho gz$, of Euler equation we have $\Phi=-\dfrac{1}{\rho}\lim\limits_{\delta t\to 0}\int_0^{\delta t}p\mathrm{d}t$. Ignoring gravity we have the following formulas:

$$\begin{aligned}&p=-\rho\frac{\partial\Phi}{\partial t}=-\rho\int_S\frac{\dot{\psi}(P)}{r_{PM}}\mathrm{d}S_P,\\&2\pi\dot{\psi}(M_S)=\int_S\dot{\psi}(P)\frac{\cos(r_{PM_S},n_{M_S})}{r_{PM_S}^2}\mathrm{d}S_P+\dot{V}_n(M_S),\end{aligned}\tag{3}$$

where $\psi(P)$ is the intensity of point source, V_n is the normal velocity of body surface, and r_{PM} is the distance from point P to M.

The normal components of velocity and acceleration of point P in the perpendicular cross section at x can be respectively written as:

$$\begin{aligned}V_n=&-\left[U(t)+\frac{\partial u(x,t)}{\partial t}\right]\sin\phi(x)\\&+\left[W(t)+\frac{\partial w(x,t)}{\partial t}\right]\cos\phi(x)\cos\gamma\\&-[a(x)\sin\phi+x\cos\phi(x)]\dot{\vartheta}(t)\cos\gamma,\end{aligned}\tag{4a}$$

$$\begin{aligned}\dot{V}_n=&-\left[\dot{U}(t)+\frac{\partial^2 u(x,t)}{\partial t^2}\right]\sin\phi(x)\\&+\left[\dot{W}(t)+\frac{\partial^2 w(x,t)}{\partial t^2}\right]\cos\phi(x)\cos\gamma\\&-[a(x)\sin\phi+x\cos\phi(x)]\ddot{\vartheta}(t)\cos\gamma,\end{aligned}\tag{4b}$$

where U and W are the velocity components of rigid motions respectively in the x axis and the z axis.

Eqs. (4a) and (4b) indicate that V_n (or $\dot{V}_n$) consists of three rigid motions of cross section at x, i.e. axial translation, transverse translation and rotation motion around the y axis. Therefore three corresponding fluid fields should be solved to obtain fluid pressures and potential functions. Here a body segment, vertical to the symmetric axis at $x=x_0$ and with $\mathrm{d}x_0$ length, is considered. The segment is assumed to move with 1 unit acceleration of translation and rotation around the y axis respectively, while other parts of the body remain static. Then by the superposition principle the potential functions of the three motions are derived and superimposed as the final solution. The source function of point (x,r,γ) on the body surface is written as

$$\begin{aligned}\mathrm{d}\psi(x,\gamma,t;x_0)=&\left[\dot{U}(t)+\frac{\partial^2 u(x_0,t)}{\partial t^2}\right]\pi_x(x;x_0)\mathrm{d}x_0\\&+\left[\dot{W}(t)+\frac{\partial^2 w(x_0,t)}{\partial t^2}\right]\pi_z(x,\gamma;x_0)\mathrm{d}x_0\\&+\ddot{\vartheta}(t)\pi_\vartheta(x,\gamma;x_0)\mathrm{d}x_0,\end{aligned}\tag{5}$$

where π_x,π_z and π_ϑ, depending on the geometry shape of segment element at $x=x_0$ together with the whole body, are solutions to the following equation, respectively:

$$\begin{aligned}2\pi\pi_x(x,x_0)=&-\int_{-a}^{b}\frac{\pi_x(x',x_0)a(x')}{\cos\phi(x')}\int_0^{2\pi}\frac{f_1}{f_2}\mathrm{d}\gamma'\mathrm{d}x'\\&-\Delta\sin\phi(x_0),\end{aligned}\tag{6a}$$

$$\begin{aligned}2\pi\pi_z(x,\gamma,x_0)=&-\int_{-a}^{b}\frac{a(x')}{\cos\phi(x')}\int_0^{2\pi}\frac{\pi_z(x',\gamma',x_0)f_1}{f_2}\mathrm{d}\gamma'\mathrm{d}x'\\&+\Delta\cos\phi(x_0)\cos\gamma,\end{aligned}\tag{6b}$$

$$\begin{aligned}2\pi\pi_\vartheta(x,\gamma,x_0)=&-\int_{-a}^{b}\frac{a(x')}{\cos\phi(x')}\int_0^{2\pi}\frac{\pi_\vartheta(x',\gamma',x_0)f_1}{f_2}\mathrm{d}\gamma'\mathrm{d}x'\\&-\Delta[a(x_0)\sin\phi(x_0)+x_0\cos\phi(x_0)]\cos\gamma,\end{aligned}\tag{6c}$$

$x_0-\mathrm{d}x_0/2\leqslant x\leqslant x_0+dx_0/2$, $\Delta=1$, otherwise $\Delta=0$.

f_1 and f_2 are

$$\begin{aligned}f_1=&-(x-x')\sin\phi(x)+a(x)\cos\phi(x)\\&-a(x')\cos\phi(x)\cos(\gamma-\gamma'),\\f_2=&[(x-x')^2+a^2(x)+a^2(x')\\&-2a(x)a(x')\cos(\gamma-\gamma')]^{3/2}.\end{aligned}$$

Substituting eq. (5) into pressure formula eq. (3) and decomposing π_z and π_ϑ into forms of $\pi_z(x,\gamma,x_0)=\Pi_z(x,x_0)\cos\gamma$ and $\pi_\vartheta(x,\gamma,x_0)=\Pi_\vartheta(x,x_0)\cos\gamma$, respectively, hydrodynamic pressures on the body surface produced by the three rigid motions are given as follows:

$$p^x(x)=-\rho\int_{-a}^{b}\left[\dot{U}(t)+\frac{\partial^2 u(x_0,t)}{\partial t^2}\right]K^x(x,x_0)\mathrm{d}x_0,\tag{7}$$

$$p^z(x,\gamma)=-\rho\cos\gamma\int_{-a}^{b}K^z(x,x_0)\left[\dot{W}(t)+\frac{\partial^2\dot{w}(x_0,t)}{\partial t^2}\right]\mathrm{d}x_0,\tag{8}$$

$$p^\vartheta(x,\gamma)=-\rho\ddot{\vartheta}\cos\gamma\int_{-a}^{b}K^\vartheta(x,x_0)\mathrm{d}x_0.\tag{9}$$

Kernel functions $K^x(x,x_0)$, $K^z(x,x_0)$ and $K^\vartheta(x,x_0)$ in the above formulas are

$$K^x(x,x_0)=\int_{-a}^{b}\pi_x(x',x_0)\frac{a(x')}{\cos\phi(x')}\int_0^{2\pi}\frac{\mathrm{d}\gamma'}{r_{0\rightarrow}}\mathrm{d}x', \tag{10}$$

$$K^z(x,x_0)=\int_{-a}^{b}\frac{\Pi_z(x',x_0)a(x')}{\cos\phi(x')}\int_0^{2\pi}\frac{\cos\gamma'\mathrm{d}\gamma'}{r_0}\mathrm{d}x'', \tag{11}$$

$$K^{\vartheta}(x,x_0)=\int_{-a}^{b}\frac{\Pi_{\vartheta}(x',x_0)a(x')}{\cos\phi(x')}\int_0^{2\pi}\frac{\cos\gamma'\mathrm{d}\gamma'}{r_0}\mathrm{d}x', \tag{12}$$

where

$$r_{0\rightarrow}=[(x-x')^2+a^2(x)+a^2(x')-2a(x)a(x')\cos(\gamma-\gamma')]^{1/2},$$

$$r_0=[(x-x')^2+a^2(x)+a^2(x')-2a(x)a(x')\cos\gamma']^{1/2}.$$

Integrating eqs. (7)–(9) can yield the total pressure field.

It should be pointed out that for many submarine bodies in practical engineering such as submarine launched missile, the acceleration of rigid motion is much smaller than the acceleration of elastic vibration, or the character time for rigid motion is much longer than the period of elastic vibration. Therefore those terms for motions with a short period can be neglected when pressure equations are substituted into kinematics equation eq. (1). Similarly terms for motions with a long period can be neglected when pressure equations are substituted into dynamics equation eq. (2).

2.3 Governing equations and added mass

Further, the acceleration $(\ddot{X},\ddot{Z})$ is projected onto the *x*-*z* coordinate, and eqs. (1a)–(1c) are rewritten as:

$$(M+M_x)\dot{U}=-Mg\sin\vartheta, \tag{13}$$

$$(M+M_z)\dot{W}=-Mg\cos\vartheta, \tag{14}$$

$$(J+J_a)\ddot{\vartheta}-\alpha M_z L\dot{W}=0, \tag{15}$$

where the expressions for added mass are:

$$M_x=2\pi\rho\int_{-a}^{b}\sin\phi(x)\int_{-a}^{b}\Gamma^x(x,x_0)\mathrm{d}x_0\mathrm{d}x,$$

$$M_z=\pi\rho\int_{-a}^{b}\cos\phi(x)\int_{-a}^{b}\Gamma^z(x,x_0)\mathrm{d}x_0\mathrm{d}x,$$

$$J_a=\pi\rho\int_{-a}^{b}a_{ax}\int_{-a}^{b}\Gamma^{\vartheta}(x,x_0)\mathrm{d}x_0.$$

And the coupling term in eq. (15) is

$$\alpha M_z L=\pi\rho\int_{-a}^{b}a_{ax}\int_{-a}^{b}\Gamma^z(x,x_0)\mathrm{d}x_0\mathrm{d}x,$$

where L is the total length of body. The above formulas imply that the two equations of translation motions are decoupled with each other, while the rotation motion is coupled with the transverse motion because of position difference between the mass center of body and the acting center of hydrodynamic force produced by the transverse motion.

By now the dynamic equations can be rewritten as:

$$\begin{aligned}&m\frac{\partial^2 u}{\partial t^2}+m\frac{\partial\vartheta}{\partial t}\frac{\partial w}{\partial t}\\&=K(x)\frac{\partial^2 u}{\partial x^2}-\frac{1}{2}\frac{\partial}{\partial x}K(x)\left(\frac{\partial w}{\partial x}\right)^2\\&\quad-2\pi\rho\cos\phi(x)\int_{-a}^{b}\frac{\partial^2 u(x_0,t)}{\partial t^2}\Gamma^x(x,x_0)\mathrm{d}x_0,\end{aligned} \tag{16a}$$

$$\begin{aligned}&m\frac{\partial^2 w}{\partial t^2}-m\frac{\partial\vartheta}{\partial t}\frac{\partial u}{\partial t}\\&=-\frac{\partial^2}{\partial x^2}\left[H(x)\frac{\partial^2 w}{\partial x^2}\right]-\frac{\partial}{\partial x}K(x)\frac{\partial u}{\partial x}\frac{\partial w}{\partial x}\\&\quad-\pi\rho\cos\phi(x)\int_{-a}^{b}\Gamma^z(x,x_0)\frac{\partial^2\dot{w}(x_0,t)}{\partial t^2}\mathrm{d}x_0.\end{aligned} \tag{16b}$$

Apparently, terms like $+m\frac{\partial\vartheta}{\partial t}\frac{\partial w}{\partial t}$, $-\frac{1}{2}\frac{\partial}{\partial x}K(x)\left(\frac{\partial w}{\partial x}\right)^2$, $-m\frac{\partial\vartheta}{\partial t}\frac{\partial w}{\partial t}$ and $-\frac{\partial}{\partial x}K(x)\frac{\partial u}{\partial x}\frac{\partial w}{\partial x}$ make the above two equations nonlinearly coupled. And eq. (16) can be further linearized based on the assumption of small deformation.

Now we have come up with the following two outlooks on the hydrodynamic force and coupling characteristics of governing equations: (1) The hydrodynamic pressure consists of two parts. The first part, produced by rigid motions, is the sum of one axisymmetric pressure by longitudinal translation acceleration and pressures, distributing on the circle according to $\cos\gamma$ function, by the transverse translation acceleration and rotation acceleration. The second part, produced by elastic deformation vibration, is the superposition result of an axisymmetric pressure by longitudinal vibration acceleration and a pressure, distributing on the circle according to $\cos\gamma$ function, by the transverse vibration acceleration. Hydrodynamic pressure derived as the above can be expressed in terms of added mass multiplying the corresponding body surface acceleration; (2) Generally, three rigid motions and two elastic deformation vibrations are coupled by hydrodynamic pressure. For some practical engineering problems the character time for rigid motion is much longer than the period for elastic vibration. Therefore equations both for rigid motions and elastic vibrations can be decoupled except one, eq. (15), where the rotation motion is still coupled with the transverse motion.

3 Example and discussion

3.1 Example and model description

A cylinder shell with a cone cap, the finite element model shown in Figure 4, is taken as an illustrative example. The geometry parameters are: radius R=0.25 m, and length L=3.3 m. Vertical height of the cone cap h=0.2 m. The material properties are: bending stiffness $EI = 9.8\times10^9$ N/m^2, and Poisson's ratio 0.3. The non-dimensional mass $m^i_{\text{sta}}/m_{\text{Max}}$ (m^i_{sta} is the structure mass at ith longitudinal position, m_{Max}=54.7 kg) distributions are shown in Figure 5. The mass density of fluid ρ=1000 kg/m^3.

3.2 Calculation results

Two cases, i.e. a whole body is immerged into water (called Case A in the later section) and the back half part of a body immerged into water (Case B), are considered. Hydroelastic dynamic characteristics, i.e. vibration frequencies and modes, for the two cases are calculated. And dynamic characteristics for the dry case (whole body in air) are also calculated for comparison. Here the effect of free surface is not taken into account. For a typical representation, the selected mode shapes of cylinder shell, the three rigid modes and the first three bending modes for Case A are shown in Figure 6.

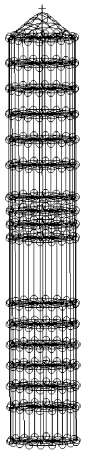

Figure 4 The finite element simulation model.

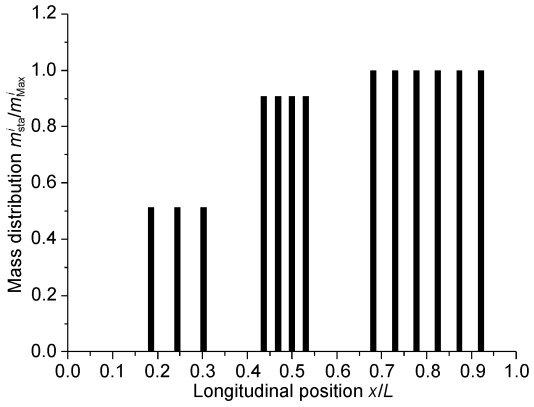

Figure 5 Sketch of the structure mass distributions.

Frequencies of dry modes and wet modes (for Cases A and B) are listed in Table 1. Generally, due to the effect of added mass, frequencies of wet modes are smaller than those of dry modes. And compared to Case B, a more pronounced frequency decrease is observed for Case A because of greater added mass caused by a larger area of body surfaces interacting with the surrounding fluid. For example, the 1st bending frequency for case A is 67% of that for the dry mode, and for Case B, 90%.

The influence of added mass, essentially implying the fluid-structure interaction, on the wet modes depends on the particular mode shape. For example, the added mass for longitude tension, whose order number is 2 for the dry case (see Table 1), is very small so that the wet frequency remains almost the same with a dry frequency, 98 Hz. The added mass of the 2nd bending, whose order number is 3 for the dry case, is large. Thereby its frequency drops from 114.6 Hz for the dry case to 84.6 Hz for the wet (Case A). It is also noted that the order number of the 2nd bending changes from 3 into 2. That is to say, compared to the dry case, the order number for a mode may change due to different degrees of influence of added mass. This can also be seen from the values of frequency ratio of wet frequency to dry frequency (see Table 1), e.g. 0.67, 0.74, 0.74, 1.00 respectively for the three bending modes and longitude tension. We know that different modes have different wave lengths, which is responsible for the degrees of influence of added mass on wet modes.

Mode shapes for the dry and wet cases are compared in Figure 7 as deformation curves of central axis. Compared to the dry case, for Case A the rotation center of rigid rotation moves forward and the vibration amplitude at the body tail augments a little (Figure 7(a)) due to a change of mass distribution. Note here that the structure mass (without added mass) is mainly at the back part of the body (Figure 5). Thus the vibration amplitude is smaller than that of the body head. But for Cass A, added mass distribution is nearly uniform along the axial length, so the total mass distribution tends to be more uniform than that of the dry case and consequently the vibration amplitude at the body tail augments. For Case B added masses are mainly at the back half part of the body, which makes back part further heavier than the front part, and consequently vibration amplitude at the back part is much smaller.

3.3 Discussion

3.3.1 A comparison with the experimental results

In practical engineering, frequency experiment is often implemented to obtain the value of added mass for a subma-

Table 1 A mode comparison for the dry and wet (Case A and B) cases (Frequency unit: Hz)

Modes	Dry case		Case A (totally submarine)			Case B (half submarine)		
	Frequency	Order number	Frequency	Order number	Frequency ratio	Frequency	Order number	Frequency ratio
1st bending	52.5	1	35.0	1	0.67	47.3	1	0.90
2nd bending	114.6	3	84.6	2	0.74	100.8	3	0.88
3rd bending	168.7	5	124.8	4	0.74	162.0	5	0.96
Longitude tension	98.0	2nd	97.9	3rd	1.00	98.0	2nd	1.00

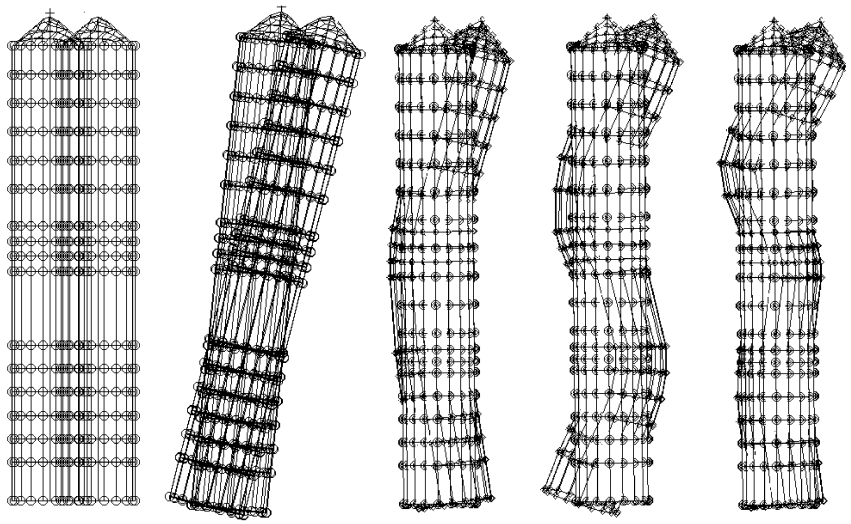

Figure 6 Hydroelastic modes for Case A (from left to right respectively: transverse translation, rotational motion; 1st, 2nd and 3rd bending modes).

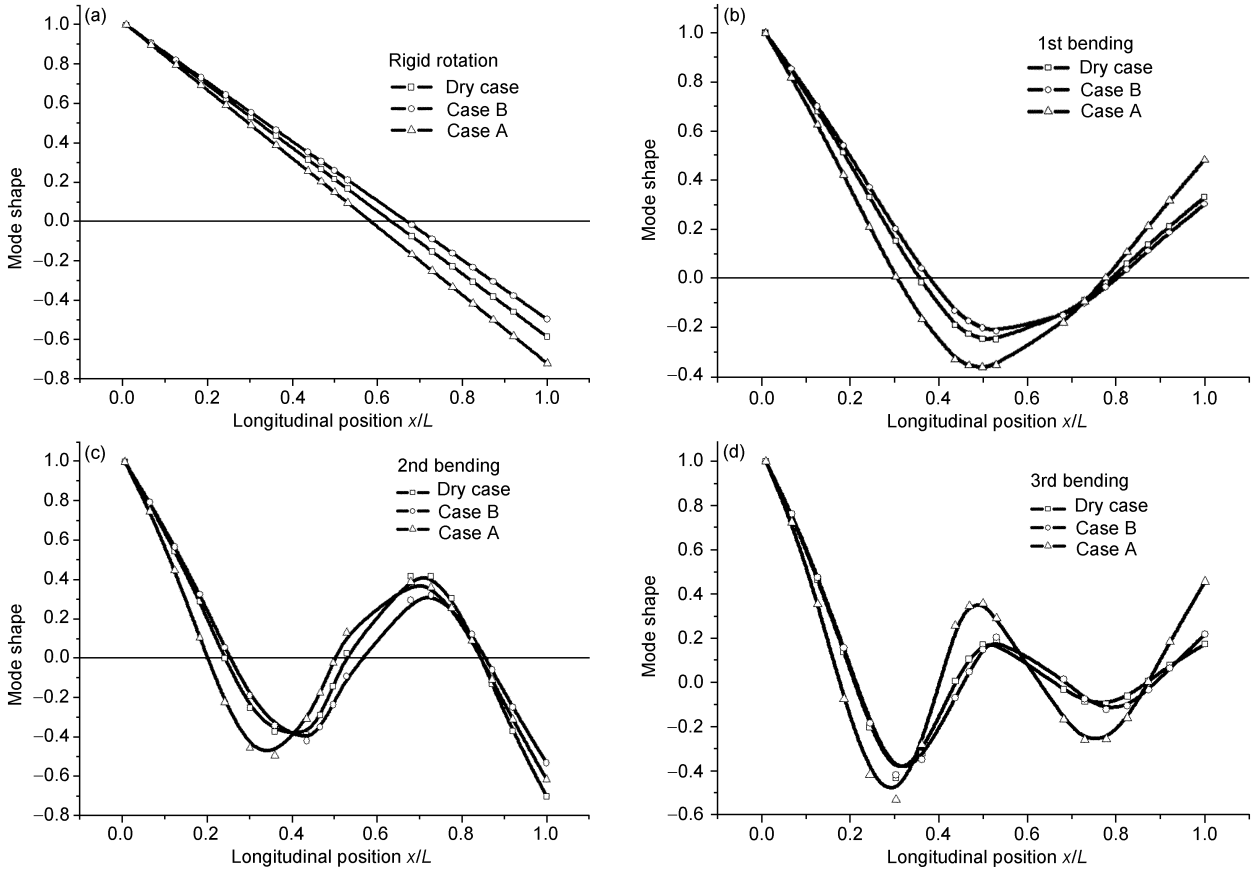

Figure 7 A comparison of mode shape for the dry and wet cases (Cases A and B). (a) Rigid rotation; (b) 1st bending; (c) 2nd bending; (d) 3rd bending.

rine body. The body is supported by a spring with stiffness $\bar{K}$, and then the frequencies for the body-spring system vibrating respectively in air and static water are measured. It is assumed that the value of spring stiffness in water is the same as that in air and the body is rigid. The influence of hydrodynamic force is considered only as an inertial force, or the effect of added mass. Therefore the frequency is related to the mass by

$$\frac{f_{\text{dry}}}{f_{\text{wet}}}=\frac{\sqrt{\bar{K}/\bar{M}_{\text{dry}}}}{\sqrt{\bar{K}/\bar{M}_{\text{wet}}}}=\sqrt{\frac{\bar{M}_{\text{wet}}}{\bar{M}_{\text{dry}}}}, \tag{17}$$

where f_{dry} and f_{wet} are the natural frequencies respectively in air and water. $\bar{M}_{\text{dry}}$ and $\bar{M}_{\text{wet}}$ are the generalized mass in air and water respectively, and satisfy $\bar{M}_{\text{wet}} = \bar{M}_{\text{dry}} + \bar{M}_{\text{a}}$ where $\bar{M}_{\text{a}}$ is the generalized added mass. For the rigid motion mode with displacement normalization, generalized mass $\bar{M}_{\text{dry}}$ (having the same value with the structure mass) is known and frequencies f_{dry} and f_{wet} can be measured by vibration experiments. Thus generalized added mass $\bar{M}_{\text{a}}$ (having same value with added mass) is calculated by

$$\bar{M}_{\text{a}}=\bar{M}_{\text{dry}}\left[\left(\frac{f_{\text{dry}}}{f_{\text{wet}}}\right)^2-1\right]. \tag{18}$$

Here the added mass coefficient C_{a} is defined as:

$$C_{\text{a}}=\frac{\bar{M}_{\text{a}}}{\bar{M}_{\text{dis}}}, \tag{19}$$

where $\bar{M}_{\text{dis}}$ is the displaced mass of body. Here the added mass coefficients C_{a}, for rigid translations, by experiments and numerical simulations are listed in Table 2. It shows that added mass coefficients by numerical simulations have a value of 0.89, and agree well with the value, 0.90, by experiment. The theoretical solution to the circular cylinder, 1.0, is compared with our numerical simulations. Significant errors, respectively 12.4% for Case A and 19.1% for Case B, are observed.

3.3.2 Effect of body end on added mass (or 3D effect)

Generally, frequency experiment in practical engineering is capable of giving a single value of added mass coefficient for a rigid mode, but hard to give added mass distribution in the body. Numerical simulations are capable of giving added mass and its distribution both for rigid modes and elastic modes. Selected results of added mass distribution (for the 1st and the 2nd bendings) along the body length are shown in Figure 8.

It shows that added mass coefficients almost keep constant along the middle part of the body length, since the end effect is negligible and the body can be regarded as an infinite length or a 2D model is acceptable. More specifically, along the length of x/L=0.20–0.79, or 59% of the total body length, the added mass coefficients C_{a} keep constant values, i.e. 0.98 and 0.95 respectively for the 1st and 2nd bending modes. But approaching the two body ends, the added mass coefficients decrease mainly due to a body end effect. It means that the 2D model for an infinitely long body no longer applies, and should be replaced by a 3D model such as presented in this paper.

4 Conclusions

A coupled model, taking into account of the interaction between fluid dynamics and structure dynamics, for a slender

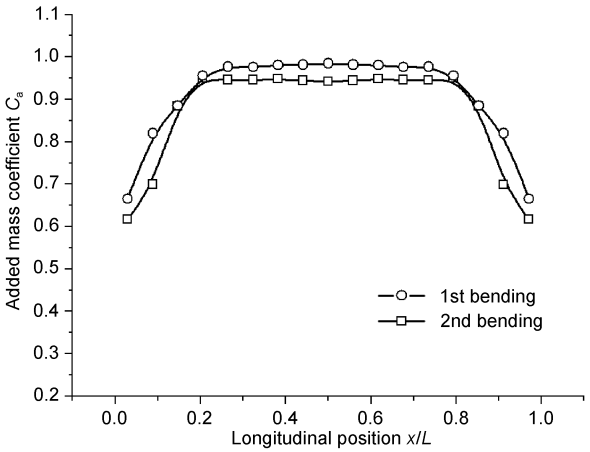

Figure 8 Added mass distributions of the wet modes (for the 1st and 2nd bending modes).

Table 2 Added mass coefficients by numerical simulations and experiments (Mass unit: kg)

Natural mode		Dry case	Case A		Case B	
		Generalized mass $\bar{M}_{\text{dry}}$	Generalized mass $\bar{M}_{\text{wet}}$	Added mass coefficient C_{a}	Generalized mass $\bar{M}_{\text{wet}}$	Added mass coefficient C_{a}
Numerical simulation results	Transverse translation (the Z direction)	612.5	1164.0	0.89	868.8	0.83
	Transverse translation (the Y direction)	612.5	1164.0	0.89	868.8	0.83
Theoretical solution (for an ideal cylinder)				1.00		1.00
Experimental results				0.90		

axis-symmetric body is studied in this paper. The governing equations are solved by means of a finite element numerical method. An illustrative example is presented, in which the hydroelastic dynamic characteristics, i.e. the natural frequencies and modes, of a submarine body are analyzed and compared with the experimental results. Satisfactory agreement is observed. Our results show:

(1) Hydrodynamics pressure, depending on and meantime conversely influencing body motions, consists of two parts. The first part is produced by rigid motions, i.e. two translations and one rotation. The second part is produced by elastic vibration in the longitudinal and transverse direction. Hydrodynamic pressure can be described in terms of added mass and the acceleration on the body surface (the expressions are presented in this paper);

(2) Generally, three rigid motions and two elastic vibrations are coupled because of expressions for hydrodynamic pressure. But for some practical engineering problems the character time for rigid motion is much longer than the elastic vibration period. Therefore equations both for rigid motion and elastic vibration can be decoupled except one (eq. (15));

(3) Frequencies for hydroelastic modes drop due to the effect of added mass whose value and influencing manner depend on a particular mode shape. Additionally the end effect of added mass is shown, which is essentially due to the 3D effect of the body shape.

This work is based on several simplifying assumptions, e.g. body moving in the vertical plane, the deformation satisfying Euler beam condition and fluid being ideally not compressible. Further works, body three-dimensional motion and more complex fluid such as vacation, separation and turbine, are suggested.

This work was supported by the National Natural Science Foundation of China (Grant No. 10772183), the Intellectual Innovation Project of the Chinese Academy of Sciences (Grant No. KJCX2-YW-L07) and the National High Technology Research and Development Program of China (Grant No. 2006AA09A103-4). The authors would like to thank Professors Zheng Zhemin and Liang Naigang for fruitful discussions.

1 Bishop R E D, Price W G. Hydroelasticity of Ships. Cambridge: Cambridge University Press, 1979
2 Bishop R E D, Price W G, Wu Y S. A general linear hydroelasticity theory of floating structures moving in a seaway. Phil Trans Royal Soc London, 1986, A316: 375–426
3 Chen X J, Wu Y S, Cui W C. Second order nonlinear hydroelastic analyses of floating bodies-theory (in Chinese). Ship Mech, 2002, 6: 21–33
4 Bai X Z, Hao Y J. Advances in nonlinear hydroelasticity (in Chinese). Adv Mech, 2008, 25: 326–331
5 Li X M, Zhang J H. A simulation analysis for frequencies of marine shell-column (in Chinese). Chin J Appl Mech, 2008, 25: 326–331
6 Zheng Z M. Plate vibration in fluid (in Chinese). Acta Mech Sin, 1958, 2: 11–16
7 Zhang X C, Sima C, Wu Y S. Low-speed flutter phenomenon of submarine rudder and its prediction (in Chinese). Ship Mech, 2001, 5: 70–72
8 Xia L, Wu W, Wang C. Analysis of fluid-structure-coupled vertical vibration for high-speed ships (in Chinese). J Ship Mech, 2000, 4: 43–50
9 Gu M X, Wu Y S, Xia J Z. Time domain analysis of non-linear hydroelastic response of ships. In: Proc. Of 4th PRADS, Varna, Bulgaria, 1989
10 Wang Z H, Xia J Z. Time domain simulation of hydroelastic response of ship in waves (in Chinese). Shipbuilding China, 1995, 4: 91–96
11 Gu X K, Duan W Y. Nonlinear hydrodynamic pressures on ship hulls in waves (in Chinese). Ship Mech, 2001, 5: 41–47
12 Sima C, Zhang X C, Wu Y S. Applications of oseenlet boundary element method in viscous fluid-structure coupling motion problems. J Ship Mech, 3: 35–39
13 Chen X J, Wu Y S, Cui W C. Second order nonlinear hydroelastic analyses of floating bodies—Effect of second order forces to time responses of vibration (in Chinese). Ship Mech, 2003, 7: 11–20
14 Du S X. A general theory for the hydroelastic response of a structure manoeuvring in viscous fluid. J Ship Mech, 1999, 3: 21–34
15 Zhang X, Lu M W, Wang J. Research progress in arbitrary Lagranian-Eulerian method (in Chinese). Chin J Comput Mech, 1997, 14: 91–102
16 Xu G, Ren W M, Zhang W, et al. Dynamic characteristic analysis of liquid-filled tanks as a 3-D fluid-structure coupling system (in Chinese). Acta Mech Sin, 2004, 36: 328–335